European Journal of Medicinal Chemistry 63 (2013) 76–84

Contents lists available at SciVerse ScienceDirect

European Journal of Medicinal Chemistry

journal homepage: http://www.elsevier.com/locate/ejmech

Original article

Platinum(II) complexes with mono-aminophosphonate ester targeting group that induce apoptosis through G1 cell-cycle arrest: Synthesis, crystal structure and antitumour activity

Ke-Bin Huang [a,b], Zhen-Feng Chen [b,*], Yan-Cheng Liu [b], Zhu-Quan Li [b], Jian-Hua Wei [b], Meng Wang [b], Guo-Hai Zhang [b], Hong Liang [a,b,*]

[a] School of Chemistry of Nankai University, Tianjin 300071, PR China
[b] Guangxi Key Laboratory for the Chemistry and Molecular Engineering of Medicinal Resources, School of Chemistry & Chemical Engineering of Guangxi Normal University, Guilin 541004, PR China

ARTICLE INFO

Article history:
Received 26 October 2012
Received in revised form
15 January 2013
Accepted 25 January 2013
Available online 9 February 2013

Keywords:
Mono-aminophosphonate ester
Platinum(II) complexes
Synthesis
Crystal structure
Cytotoxicity

ABSTRACT

Six new platinum(II) complexes with mono-aminophosphonate ester were synthesized and characterized by elemental analysis, ^{1}H NMR, ESI-MS as well as single crystal X-ray diffraction analysis. They are mononuclear structures. In all the crystal structures of complexes **1**–**6**, the platinum centre adopts an approximately square-planar geometry, which were found to possess excellent solubility in both organic solvents and water and exhibit considerable cytotoxicity against MG-63, SK-OV-3 and HepG2 cell lines, but low cytotoxicity towards normal human liver cell HL-7702. In contrast to cisplatin, their antitumour activities are achieved through the induction of cell apoptosis by G1 cell-cycle arrest.

1. Introduction

Cisplatin is one of the most widely used anti-cancer drugs [1,2], but it also has apparent clinical drawbacks including limited applicability, acquired resistance, and serious side effects such as neurotoxicity and nephrotoxicity [3–5]. These shortcomings are closely related to the lack of tumour selectivity of cisplatin [6,7], which makes it necessary to design new platinum-based compounds that are able to accumulate in specific target organs or cells and overcome the side effects of cisplatin [8,9]. In the past two decades, several design strategies have been tried to include targeting groups such as small molecule ligands and drug delivery systems into platinum-based compounds [10–14]. Because alkaline phosphatase is known to be overexpressed in the extracellular space of specific tumour cells such as ovarian and hepatic carcinoma cells, introducing a phosphate group for targeted delivery appears to be a reasonable strategy to increase solubility and enhance transport through cellular membrane [15,16]. Some phosphate groups also exhibit high affinity to calcium ions and have been used to design targeted drugs for bone cancer [17,18].

Aminophosphonic acids are structural analogues of natural aminocarboxylic acid. The functionalized aminophosphonic acids, α-aminoalkyl-phosphonic derivatives, are a class of important compounds that exhibit intriguing biological activities in the pharmacological and agrochemical fields [19–22]. Moreover, some aminophosphonic acids inhibit bone resorption, delay the progression of bone metastases, exert direct cytostatic effects on a variety of human tumour cells and have found clinical application in the treatment of bone disorders and cancer [23,24]. Polymeric aminophosphonate analogues are used as bone seeking radiopharmaceuticals [23,25]. Since phosphonate esters can be hydrolyzed under biological conditions, aminophosphonate esters are a good choice in designing targeted anti-cancer drug [26,27]. Recently, new functional ligands have been designed as leaving or non-leaving groups to coordinate with antitumour compounds and make targeted drugs [28–30]. According to the action mechanism of cisplatin under biological conditions, if the functional moieties are attached to

* Corresponding authors. Guangxi Key Laboratory for the Chemistry and Molecular Engineering of Medicinal Resources, School of Chemistry & Chemical Engineering of Guangxi Normal University, Guilin 541004, PR China. Tel./fax: +86 773 2120958.
E-mail addresses: chenzfgxnu@yahoo.com, chenzfubc@yahoo.com (Z.-F. Chen), hliang@gxnu.edu.cn (H. Liang).

0223-5234/$ – see front matter © 2013 Elsevier Masson SAS. All rights reserved.
http://dx.doi.org/10.1016/j.ejmech.2013.01.055

platinum centre as leaving group, they may detach during the complicated physiological process even before reaching the targeted tissues and the special function of the complexes will be lost. Therefore, it is very important to use the functional moieties as the non-leaving groups to "hook" the platinum to tissues. Platinum complexes incorporating functional phosphoric moieties were first reported by Keppler and co-workers in the early 1990s [31]. More recently, Natile, Bose and Guo also reported platinum–phosphonate complexes and found that some of them have a cytotoxic mechanism different from that of cisplatin. However, except for Guo's work, most of them attached leaving groups to the platinum centre [6,7,32,33]. In the present study, we designed and synthesized six nonclassic platinum antitumour complexes with (1) monoaminophosphonate ester ligands as non-leaving groups for delivery targeting, (2) pyridine groups to engage in Pt-binding, and (3) amides of pepper amine and homoveratryl amine analogues, which are known to induce apoptosis [34,35].

2. Results and discussion

2.1. Synthesis

The synthesis of aminophosphonate ester derivatives (L^a–L^f) was carried out starting from pyridinealdehyde, diethylacidphosphite and phenethylamine via one synthetic step (Scheme 1). These aminophosphonate ester derivatives were characterized by elemental analysis, ^{1}H NMR, ^{13}C NMR, and ESI-MS spectroscopy.

Corresponding *cis*-dichloroplatinum(II) complexes **1**–**6** were obtained by the reaction of *cis*-Pt(DMSO)$_2$Cl$_2$ and L^a–L^f in mixtures of anhydrous dichloromethane and ethanol (1:1), respectively (Scheme 2).

The synthetic platinum(II) complexes were characterized by elemental analysis, ^{1}H NMR, ESI-MS spectroscopy and single crystal X-ray diffraction analysis. In all the crystal structures of complexes **1**–**6**, the platinum centre adopts an approximately square-planar geometry in which the dihedral angle between the pyridyl ring and Pt(II) coordination plane is 9.8° (for **1**), 20° (for **2**), 18.6° (for **3**), 16.6° (for **4**), 12° (for **5**) and 9.7° (for **6**), respectively. Selected bond lengths and angles are listed in Figs. 1–3, and are within the normal range expected for Pt(II) complexes. One of the notable features is that the carbon atom linking to P forms a half chair conformation with the platinum coordination plane in all complexes, which is consistent with the steric interaction between the phosphonate ester moiety and the platinum coordination plane. The major structural distinctions among the complexes are the number of CH_2 units and the methylenedioxy or methoxy groups at the C_3 and C_4 of the benzene ring. The different CH_2 units result in different spatial separation of the benzene ring with the platinum coordination plane. Besides, in contrast to cisplatin, complexes **1**–**6** all exhibit good solubility in both organic solvents and water.

2.2. In vitro cytotoxic activity

The *in vitro* cytotoxicities of complexes **1**–**6** against MG-63, SK-OV-3, HepG2 and HL-7702 cell lines were investigated and compared with those of cisplatin. As shown in Table 1, the IC_{50} values of complexes **1**–**6** against MG-63, SK-OV-3 and HepG2 were all higher than that of cisplatin and exhibited considerable cytotoxicities. Among the reported complexes, complexes **2** and **5** showed the highest cytotoxicities against tested tumour cell lines. It should be noted that these platinum(II) complexes towards the normal human liver HL-7702 cells displayed lower cytotoxicities than that of them to the tested tumour cell lines, and also lower than that of cisplatin. Viewing from their structures, it can be presumed that a linkage of one methylene unit between the α-nitrogen of the aminophosphonate and the apoptosis-inducing benzene ring moiety is optimal for cytotoxicity, and the methylenedioxy group at the C_3 and C_4 of the benzene ring can enhance activity.

2.3. Apoptosis study by flow cytometry assay

To determine whether the observed cell death induced by the complexes was due to apoptosis or necrosis, the interaction of MG-63 cells with complexes **2** and **5** was further investigated using an Annexin V-FITC/propidium iodide assay (Fig. 4). As phosphatidylserine (PS) exposure usually precedes loss of plasma membrane integrity in apoptosis, the presence of Annexin V+/PI− cells is considered an indicator of apoptosis. In the case of complexes **2** and **5**, the population of Annexin V+/PI− cells (Q4) are 39.1% and 29.3% respectively, which suggests that apoptotic death was induced in MG-63 cells.

2.4. Cell-cycle analysis

The cell cycle is the series of events that take place in a cell leading to its division and duplication (replication). The cell cycle consists of four distinct phases: G_1 phase, S phase (synthesis), G_2 phase (collectively known as interphase) and M phase (mitosis). The G1 stage is the stage when preparation of energy and material for DNA replication occurs. The S stage is the stage when DNA replication occurs. The G2 stage is the stage when preparation for the M stage occurs. The M stage is "mitosis", and is when nuclear and cytoplasmic division occurs. To determine whether the suppression of cancer cell growth by the platinum complexes was caused by a cell-cycle arrest. The MG-63 cells were treated with complexes **2**, **5** and cisplatin at IC_{50} concentrations and the cell-cycle phases were assayed through assessing the DNA content of cells stained with propidium iodide as measured by flow cytometry (Fig. 5). As shown in Fig. 5, treatment of MG-63 cells with complexes **2**, **5** for 24 h enhanced cell-cycle arrest at the G1 phase, resulting in concomitant population increase in the G1 phase (65.05% and 62.98% for **2** and **5**,

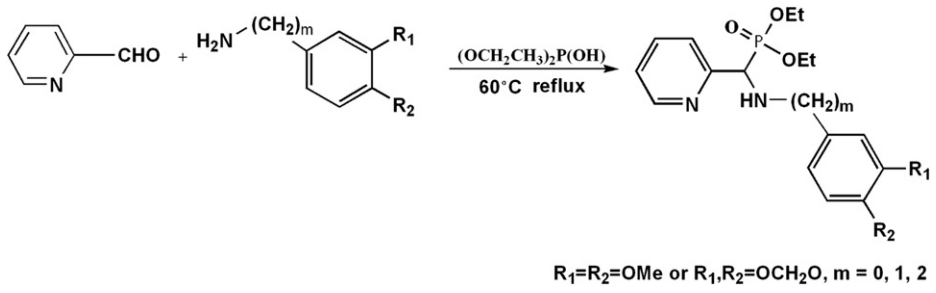

Scheme 1. Synthetic route for aminophosphonate esters.

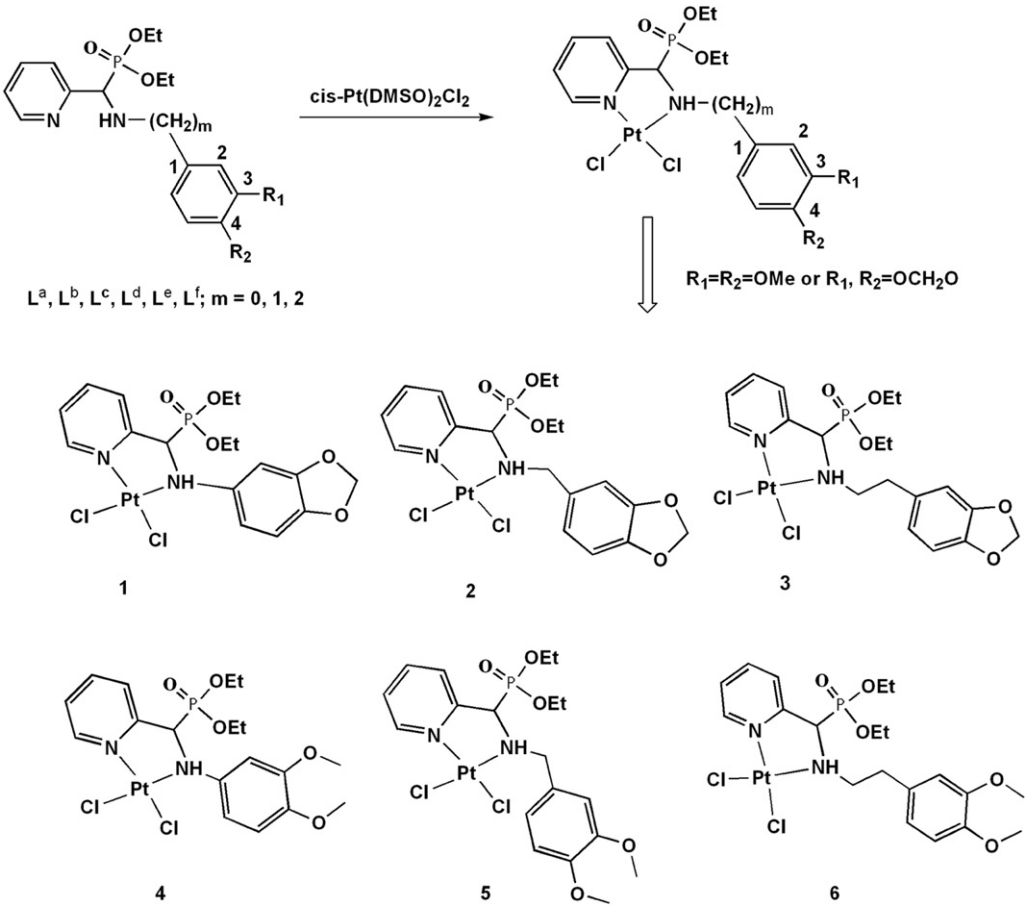

Scheme 2. Synthesis of the six platinum(II) complexes.

respectively) compared with the control cells (48.88%) and the population of the S phase decrease at a certain extent (28.47% and 31.08% for **2** and **5**, respectively) compared with the control cells (36.07%). These results suggested that the G1 stage was stopped, the preparation of energy and material for DNA replication could not occurred, and the S stage was stopped, the DNA replication was blocked. Thus the population of G2 also decreased. The G1 phase arrest could be the main reason for the population decease of S and G2 phases in MG-63 cell cycle induced by complexes **2** and **5**. Therefore, the synergistic interplay of G1 and S led to MG-63 cells apoptotic death before enter M phase. However, cisplatin resulted in the population increase in the S phase (53.95% and 36.07% for cisplatin and control, respectively), which suggested block of DNA replication was the mainly reason when cell cycles were arrested by cisplatin. The results are in agreement with the literature regarding cell-cycle arrest by cisplatin [36]. Therefore, the mechanism of the suppression of tumour cell growth by the title platinum complexes is different from that of cisplatin.

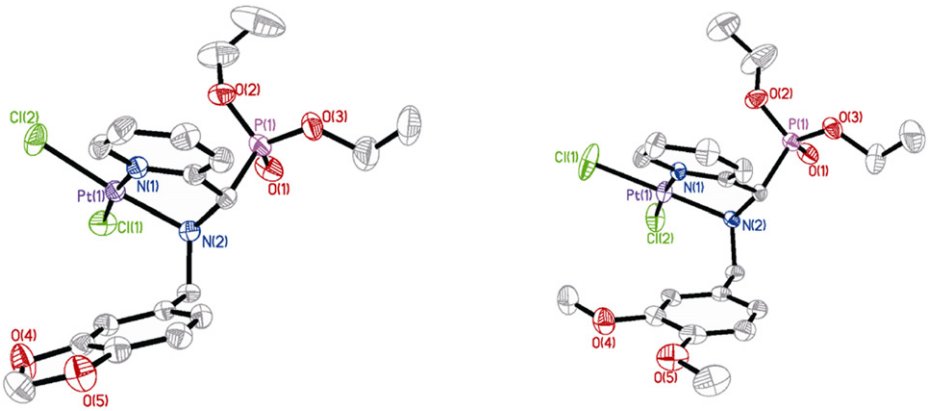

Fig. 1. ORTEP drawing of **2** (left) and **5** (right). The hydrogen atoms have been omitted for clarity. Selected bond lengths (Å) and angles (°) for **2**: Pt(1)–N(1) 2.0177(68), Pt(1)–N(2) 2.0557(59), Pt(1)–Cl(2) 2.2985(25), Pt(1)–Cl(1) 2.2996(26); N(1)–Pt(1)–N(2) 82.01(26), N(1)–Pt(1)–Cl(2) 94.02(20), N(1)–Pt(1)–Cl(1) 71.82(20), N(2)–Pt(1)–Cl(2) 174.59(19), N(2)–Pt(1)–Cl(1) 89.90(20), Cl(2)–Pt(1)–Cl(1) 94.12(11); for **5**: Pt(1)–N(1) 1.9994(40), Pt(1)–N(2) 2.0540(43), Pt(1)–Cl(2) 2.2818(15), Pt(1)–Cl(1) 2.2897(18); N(1)–Pt(1)–N(2) 82.53(17), N(1)–Pt(1)–Cl(2) 174.62(12), N(1)–Pt(1)–Cl(1) 94.71(13), N(2)–Pt(1)–Cl(2) 92.30(12), N(2)–Pt(1)–Cl(1) 177.01(12), Cl(2)–Pt(1)–Cl(1) 90.43(7).

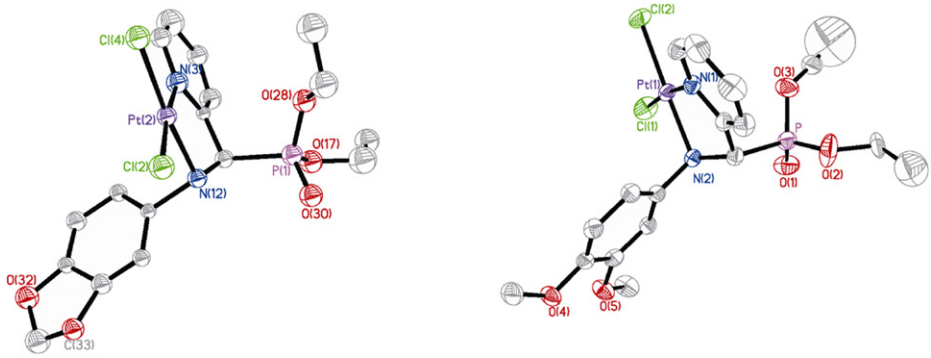

Fig. 2. ORTEP drawing of complexes **1** (left) and **4** (right), and the hydrogen atoms and solvent molecule (ethanol for **4**) have been omitted for clarity. Selected bond lengths (Å) angles (°), for **1**: Pt(2)–N(12) 2.0828(31.3), Pt(2)–N(3) 2.1394(29.6), Pt(2)–Cl(4) 2.2721(9.4), Pt(2)–Cl(2) 2.2804(11.9), N(3)–Pt(2)–N(12) 80.68(1.15), Cl(4)–Pt(2)–N(12) 174.27 (8.5), Cl(2)–Pt(2)–N(12), 91.61(8.9), N(3)–Pt(2)–Cl(4) 95.24(8.4), N(3)–Pt(2)–Cl(2) 172.14(9.4), Cl(4)–Pt(2)–Cl(2) 92.34(3.8); for **4**: Pt(1)–N(1) 2.0172(44), Pt(1)–N(2) 2.0544(38), Pt(1)–Cl(1) 2.2802(17), Pt(1)–Cl(2) 2.2941(14), N(1)–Pt(1)–N(2) 82.24(16), N(1)–Pt(1)–Cl(1) 172.93(12), N(1)–Pt(1)–Cl(2) 94.79(13), Cl(1)–Pt(1)–N(2) 90.74(12), Cl(2)–Pt(1)–N(2) 176.98(13), Cl(2)–Pt(1)–Cl(2) 92.23(7).

2.5. Interaction with pUC19 plasmid DNA

Since these platinum complexes possess the classic *cis*-dichloro coordination mode similar to cisplatin, we tried to compare their interaction with ct-DNA with that of cisplatin. As shown in the gel electrophoresis experiments (Fig. 6), at low concentrations, complexes **2** and **5** induced no significant change in the migration rate of the supercoiled pUC19 plasmid DNA. The migration rate of Form I DNA abruptly decreased when the concentration of complex **2** reached 100 μM and when the concentration of complex **5** reached 120 μM, but it then increased notably when the concentration of complex **2**, further increased to 110 μM and when the concentration of complex **5** further increased to 130 μM. In contrast, cisplatin induced no change in migration rate at concentrations below 40 μM and steadily decreased the DNA migration rate at concentrations greater than 40 μM. The results suggest that compared with cisplatin, the prepared platinum complexes have different interaction mechanism with DNA monotonously.

3. Conclusions

In conclusion, six new mononuclear platinum complexes **1**–**6** with mono-aminophosphonate esters as the non-leaving group were synthesized and fully characterized. In cytotoxicity assay against MG-63, SK-OV-3 and HepG2 cells, **2** and **5** demonstrated the best activity among the complexes, which may be correlated to (1) the length of the methylene linker between the α-nitrogen of the aminophosphonate and the apoptosis-inducing benzene ring moiety, and (2) the substitution at the C_3 and C_4 of the benzene ring. Complexes **2** and **5** induced apoptosis in tumour cells through G1 cell-cycle arrest, which is different from cisplatin that induces S phase cell-cycle arrest. The electrophoretic mobility studies revealed that the binding mode of **2** and **5** to DNA is different from that of cisplatin. This work affords a new method to obtain water soluble platinum complexes bearing mono-aminophosphonate esters as the non-leaving group and having action mechanism different from cisplatin.

4. Experimental

4.1. Materials

All chemicals, unless otherwise noted, were purchased from Sigma and Alfa Aesar. All materials were used as received without further purification unless noted specifically. Tris–HCl–NaCl (TBS) buffer solution (5 mM Tris, 50 mM NaCl, pH adjusted to 7.35 by

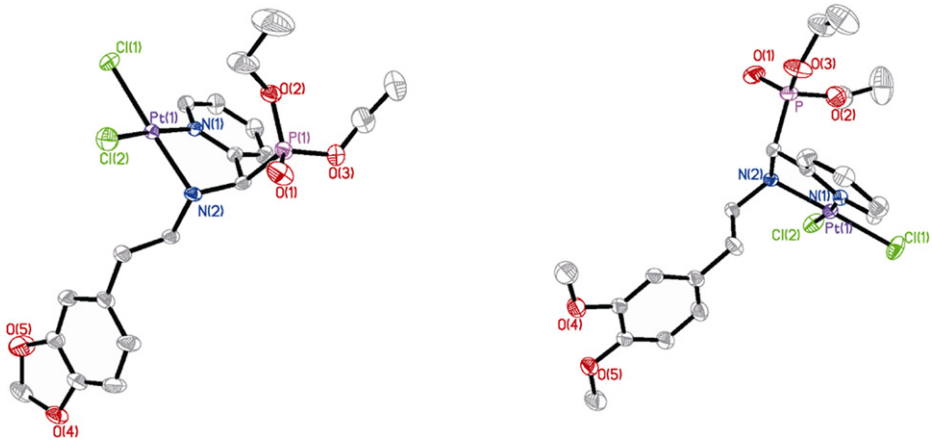

Fig. 3. ORTEP drawing of complexes **3** (left) and **6** (right), and the hydrogen atoms have been omitted for clarity. Selected bond lengths (Å) and angles (°), for **3**: Pt(1)–N(1) 2.0093(38), Pt(1)–N(2) 2.0470(36), Pt(1)–Cl(2) 2.2902(13), Pt(1)–Cl(1) 2.3008(13); N(1)–Pt(1)–N(2) 80.73(15), N(1)–Pt(1)–Cl(2) 172.44(11), N(1)–Pt(1)-Cl(1) 94.26(11), N(2)–Pt(1)–Cl(2) 93.31(11), N(2)–Pt(1)–Cl(1) 174.93(10), Cl(2)–Pt(1)–Cl(1) 91.74(5); for **6**: Pt(1)–N(1) 2.0090(32), Pt(1)–N(2) 2.0593(30), Pt(1)–Cl(2) 2.2929(15), Pt(1)–Cl(1) 2.2921(12); N(1)–Pt(1)–N(2) 82.72(12), N(1)–Pt(1)–Cl(2) 174.51(9), N(1)–Pt(1)–Cl(1) 176.63(9), N(2)–Pt(1)-Cl(2) 91.84(9), N(2)–Pt(1)–Cl(1) 176.63(9), Cl(2)–Pt(1)–Cl(1) 90.89(4).

Table 1
IC_{50} (μM) for complexes **1**–**6** against three human tumour cells.

Complex	MG-63	SK-OV-3	HepG2	HL-7702
1	28.4	38.2	33.7	109.2
2	12.7	17.6	23.4	103.9
3	>50	47.2	>50	129.9
4	34.5	28.9	40.5	152.2
5	17.9	25.8	24.2	135.3
6	>50	>50	45.2	101.0
Cisplatin[a]	9.5	6.4	11.5	85.98

[a] Cisplatin was used as positive control.

titration with hydrochloric acid using a Sartorius PB-10 pH meter, Tris = tri(hydroxymethyl)aminomethane) was prepared using double distilled water. The TBE buffer (1×) and DNA loading buffer (6×) were commercially available. Calf thymus DNA (ct-DNA) was purchased from Sino-American Biotech Co., Ltd. (Beijing). Ct-DNA gave a UV absorbance ratio at 260–280 nm of ~1.85:1, indicating that the DNA was effectively free of protein. The DNA concentration pernucleotide was determined spectrophotometrically by employing a molar absorption coefficient (6600 M^{-1} cm^{-1}) at 260 nm. The stock solution of pUC19 plasmid DNA (250 μg/mL) was purchased from Takara Biotech Co., Ltd.

4.2. Instrumentation

^{1}H NMR and ^{13}C NMR spectra were recorded on a Bruker AV-500 NMR spectrometer with $CDCl_3$ as solvent. Elemental analyses (C, H, and N) were carried out on a PerkinElmer Series II CHNS/O 2400 elemental analyzer. ESI-MS spectra for the characterization of complexes were performed on Thermofisher Scientific Exactive LC–MS Spectrometer.

4.3. Synthesis

4.3.1. Synthesis of the ligands

General procedure for the synthesis of aminophosphonate ester ligands [23]: Equimolar amounts (0.2 mol) of pyridinealdehyde, diethylacidphosphite and phenethylamine were refluxed for 1 h at 60 °C, after the reacting mixture was cooled to room temperature, the oily residue was purified on a silica gel column (petroleum ether:ethyl acetate = 1:1). Yellow oil-like product was obtained.

Data for L^a: ^{1}H NMR (500 MHz, $CDCl_3$) δ 8.57 (d, J = 4.6 Hz, 1H), 7.61 (t, J = 7.7 Hz, 1H), 7.51–7.34 (m, 1H), 7.16 (t, J = 6.0 Hz, 1H), 6.55 (d, J = 8.3 Hz, 1H), 6.30 (d, J = 2.2 Hz, 1H), 6.08 (dd, J = 8.4, 2.3 Hz, 1H), 5.78 (s, 2H), 4.85 (dd, J = 22.3, 7.3 Hz, 1H), 4.18–4.06 (m, 2H), 4.01 (dt, J = 10.0, 7.1 Hz, 1H), 3.91–3.82 (m, 1H), 1.26 (t, J = 7.1 Hz, 3H), 1.14 (t, J = 7.1 Hz, 3H). ^{13}C NMR (126 MHz, $CDCl_3$) δ 155.81 (s), 148.75 (d, J = 126.1 Hz), 148.24 (s), 142.28 (s), 142.17 (s), 140.39 (s), 136.61 (s), 122.78 (dd, J = 8.4, 3.4 Hz), 108.45 (s), 106.01 (s), 100.21 (d, J = 112.5 Hz), 97.31 (s), 63.45 (d, J = 6.9 Hz), 63.13 (d, J = 7.2 Hz), 59.68 (s), 58.47 (s), 16.42 (d, J = 5.6 Hz), 16.23 (d, J = 5.8 Hz). ESI-MS: m/z 365.12 $[L^a + H]^+$.

Data for L^b: ^{1}H NMR (500 MHz, $CDCl_3$) δ 8.57 (d, J = 3.9 Hz, 1H), 7.67–7.61 (m, 1H), 7.39 (d, J = 7.8 Hz, 1H), 7.21–7.15 (m, 1H), 6.79 (s, 1H), 6.66 (dd, J = 16.7, 7.9 Hz, 2H), 5.88 (s, 2H), 4.18–4.12 (m, 1H), 4.12–4.04 (m, 2H), 4.03–3.95 (m, 1H), 3.94–3.85 (m, 1H), 3.69 (d, J = 13.1 Hz, 1H), 3.46 (d, J = 13.0 Hz, 1H), 1.25 (t, J = 7.0 Hz, 3H), 1.14 (t, J = 7.1 Hz, 3H). ^{13}C NMR (126 MHz, $CDCl_3$) δ 156.11 (s), 149.30 (s), 147.83 (d, J = 44.7 Hz), 146.62 (s), 136.89–135.60 (m), 133.18 (s), 123.82 (d, J = 4.8 Hz), 122.45 (dd, J = 45.0, 5.2 Hz), 121.53 (s), 109.04–108.64 (m), 107.95 (s), 100.97 (d, J = 31.6 Hz), 63.17 (d, J = 6.9 Hz), 62.77 (t, J = 8.4 Hz), 61.47 (s), 59.91 (d, J = 87.9 Hz), 51.73 (d, J = 17.1 Hz), 16.40 (d, J = 5.8 Hz), 16.25 (d, J = 5.9 Hz). ESI-MS: m/z 379.13 $[L^b + H]^+$.

Data for L^c: ^{1}H NMR (500 MHz, $CDCl_3$) δ 8.53 (dd, J = 4.8, 1.4 Hz, 1H), 7.62 (td, J = 7.7, 1.6 Hz, 1H), 7.38–7.34 (m, 1H), 7.19–7.14 (m, 1H), 6.66 (d, J = 7.8 Hz, 1H), 6.60 (d, J = 1.6 Hz, 1H), 6.55 (d, J = 1.6 Hz, 1H), 5.86 (s, 2H), 4.18 (d, J = 21.3 Hz, 1H), 4.10–4.03 (m, 2H), 3.99 (dt, J = 10.0, 7.2 Hz, 1H), 3.93–3.85 (m, 1H), 2.70 (dd, J = 7.0, 5.1 Hz, 2H), 2.68–2.64 (m, 2H), 1.22 (t, J = 7.1 Hz, 3H), 1.13 (t, J = 7.1 Hz, 3H). ^{13}C NMR (126 MHz, $CDCl_3$) δ 156.34 (s), 149.18 (s), 147.51 (s), 145.80 (s), 136.41 (s), 133.58 (s), 123.43 (d, J = 4.7 Hz), 122.64 (d, J = 2.5 Hz), 121.52 (s), 108.98 (d, J = 31.2 Hz), 108.09 (s), 100.80 (d, J = 16.6 Hz), 63.28–63.00 (m), 62.79 (d, J = 7.0 Hz), 62.01 (s), 50.12 (d, J = 16.4 Hz), 35.97 (s), 16.36 (d, J = 5.8 Hz), 16.25 (d, J = 5.7 Hz). ESI-MS: m/z 379.1 $[L^c + H]^+$.

Data for L^d: ^{1}H NMR (500 MHz, $CDCl_3$) δ 8.60–8.50 (m, 1H), 7.62 (td, J = 7.7, 1.6 Hz, 1H), 7.52–7.41 (m, 1H), 7.21–7.08 (m, 1H), 6.68–6.53 (m, 1H), 6.32 (d, J = 2.6 Hz, 1H), 6.13 (dt, J = 25.5, 12.8 Hz, 1H), 4.91 (d, J = 22.5 Hz, 1H), 4.16–4.06 (m, 2H), 4.05–3.97 (m, 1H), 3.86 (tdd, J = 8.0, 4.6, 2.1 Hz, 1H), 1.26 (t, J = 7.1 Hz, 3H), 1.13 (t, J = 7.1 Hz, 3H). ^{13}C NMR (126 MHz, $CDCl_3$) δ 156.02 (s), 149.81 (s), 149.11 (s), 142.16 (s), 141.27 (s), 141.16 (s), 136.74 (s), 122.83 (dd, J = 10.7, 3.3 Hz), 112.83 (s), 104.92 (s), 100.13 (s), 63.49 (d, J = 6.9 Hz), 63.20 (d, J = 7.2 Hz), 59.40 (s), 58.20 (s), 56.50 (s), 55.67 (s), 16.41 (d, J = 5.6 Hz), 16.22 (d, J = 5.8 Hz). ESI-MS: m/z 381.15 $[L^d + H]^+$.

Data for L^e: ^{1}H NMR (500 MHz, $CDCl_3$) δ 8.59 (dd, J = 4.8, 1.1 Hz, 1H), 7.69–7.58 (m, 1H), 7.40 (ddd, J = 11.2, 6.8, 1.5 Hz, 1H), 7.22–7.13

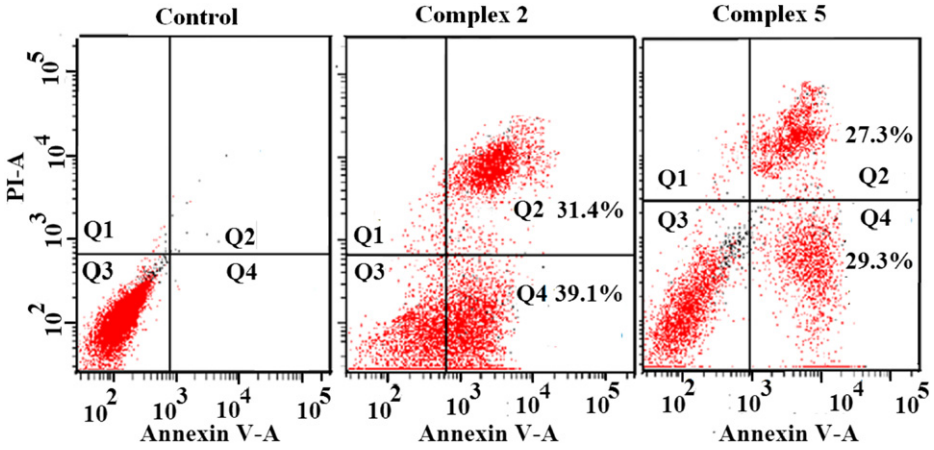

Fig. 4. Annexin V/propidium iodide assay of MG-63 cells treated by complexes **2** and **5** (at IC_{50} concentrations) measured by flow cytometry assay.

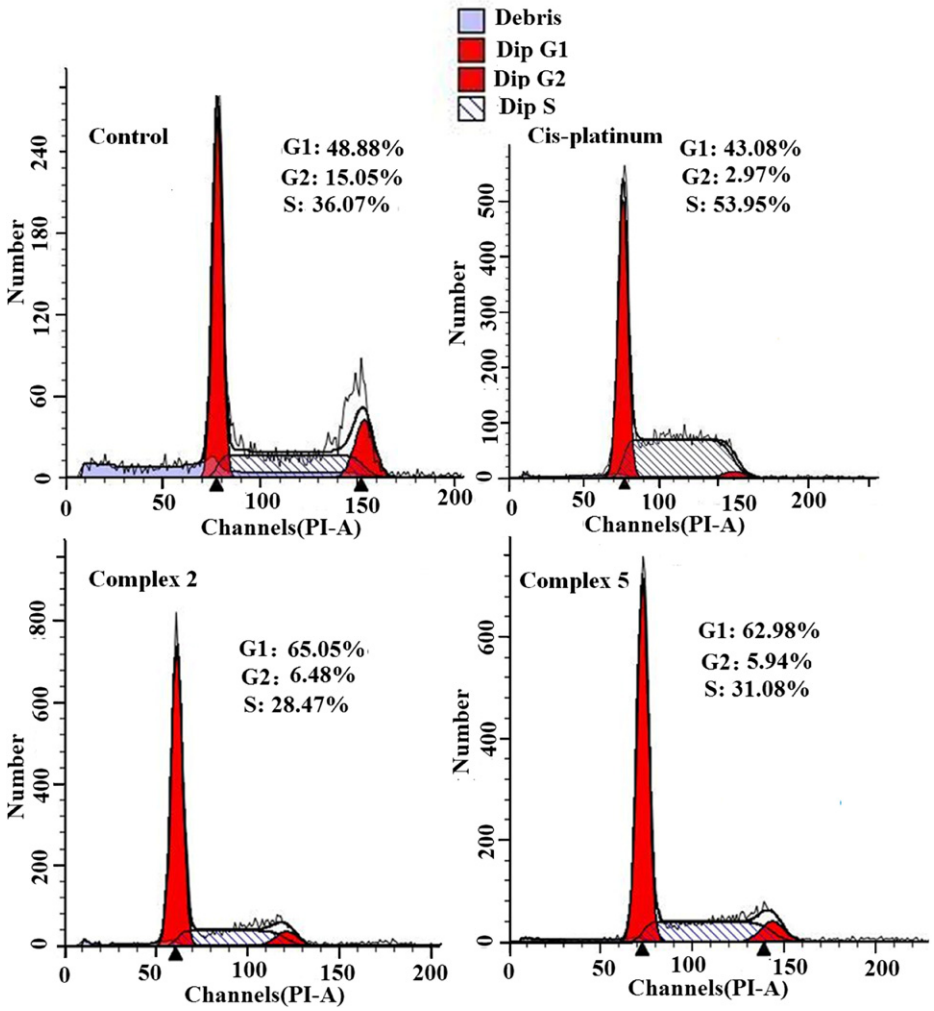

Fig. 5. Cell-cycle analysis by flow cytometry of GM-63 cells treated with complexes **2**, **5** and cisplatin at IC_{50} concentrations.

(m, 1H), 6.84 (d, J = 1.6 Hz, 1H), 6.74 (dd, J = 8.8, 4.9 Hz, 2H), 4.17 (d, J = 21.8 Hz, 1H), 4.13–4.04 (m, 2H), 4.04–3.90 (m, 2H), 3.83 (d, J = 2.5 Hz, 3H), 3.82 (s, 3H), 3.76 (d, J = 13.1 Hz, 1H), 3.52 (d, J = 13.1 Hz, 1H), 2.79 (d, J = 24.4 Hz, 1H), 1.25 (t, J = 7.1 Hz, 3H), 1.15 (t, J = 7.1 Hz, 3H). ^{13}C NMR (126 MHz, $CDCl_3$) δ 156.19 (s), 149.12 (d, J = 46.0 Hz), 148.94 (s), 148.13 (s), 136.36 (s), 131.83 (s), 123.87 (d, J = 4.8 Hz), 122.64 (d, J = 2.5 Hz), 120.59 (s), 111.47 (d, J = 31.9 Hz), 110.95 (s), 63.11 (d, J = 6.9 Hz), 62.74 (d, J = 7.0 Hz), 61.42 (s), 60.21 (s), 55.91 (s), 55.77 (s), 51.69 (d, J = 17.0 Hz), 16.42 (d, J = 5.8 Hz), 16.27 (d, J = 5.8 Hz). ESI + MS: m/z 395.19 $[L^e + H]^+$.

Data for L^f: ^{1}H NMR (500 MHz, $CDCl_3$) δ 8.52 (dd, J = 4.9, 1.5 Hz, 1H), 7.60 (td, J = 7.7, 1.7 Hz, 1H), 7.38–7.31 (m, 1H), 7.15 (ddd, J = 7.1,

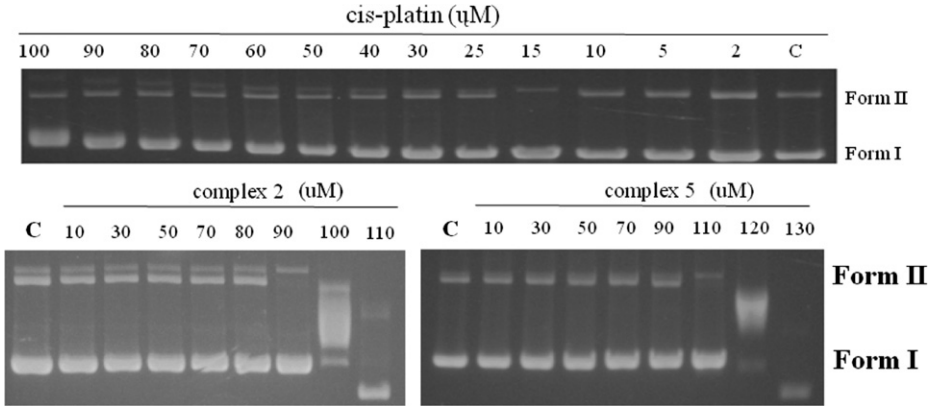

Fig. 6. Electrophoresis in agarose gel of pUC19 plasmid DNA (0.02 mg/mL, 30 μM base pair) incubated for 4 h at 37 °C with cisplatin, complexes **2** and **5**, respectively. "C" represents control; the concentration of each platinum complex is indicated in the figure.

2.8, 1.4 Hz, 1H), 6.72 (d, J = 8.0 Hz, 1H), 6.68–6.61 (m, 2H), 4.19 (d, J = 21.1 Hz, 1H), 4.11–4.03 (m, 2H), 4.00–3.93 (m, 1H), 3.88 (dd, J = 8.2, 7.1 Hz, 1H), 3.79 (s, 3H), 3.78 (s, 3H), 2.76–2.72 (m, 2H), 2.72–2.63 (m, 2H), 1.21 (t, J = 7.1 Hz, 3H), 1.12 (t, J = 7.1 Hz, 3H). ^{13}C NMR (126 MHz, $CDCl_3$) δ 156.41 (s), 148.97 (d, J = 43.0 Hz), 148.80 (s), 147.38 (s), 136.37 (s), 132.41 (s), 123.38 (d, J = 4.6 Hz), 122.60 (d, J = 2.4 Hz), 120.60 (s), 111.99 (s), 111.23 (s), 63.27 (s), 63.08 (d, J = 6.9 Hz), 62.77 (d, J = 7.0 Hz), 62.06 (s), 55.91 (s), 55.77 (s), 50.07 (d, J = 16.2 Hz), 35.83 (s), 16.35 (d, J = 5.7 Hz), 16.25 (d, J = 5.7 Hz). ESI + MS: m/z 408.12 $[L^f + H]^+$.

4.3.2. Synthesis of the platinum complexes

General procedure for the synthesis of the platinum complexes: to a solution of *cis*-$Pt(DMSO)_2Cl_2$ (84 mg, 0.2 mmol) was added L^{a-f} (0.2 mmol) dissolved in 30 mL mixtures of anhydrous dichloromethane and ethanol (1:1). The mixture was stirred in the dark at room temperature for 1 day. The resulting yellow solution was filtered and crystals were obtained by slow evaporation of filtrate solution.

Data for 1: ^{1}H NMR (500 MHz, d_6-DMSO) δ 9.31 (s, 1H), 8.32–8.19 (m, 1H), 7.56 (d, J = 7.9 Hz, 1H), 7.31–7.26 (m, 1H), 6.52 (d, J = 2.2 Hz, 1H), 6.37–6.33 (m, 1H), 6.14 (dd, J = 8.4, 2.2 Hz, 1H), 5.78 (s, 2H), 5.01 (d, J = 24.0 Hz, 1H), 4.34–4.12 (m, 1H), 4.06 (dq, J = 14.1, 7.1 Hz, 2H), 3.95–3.87 (m, 1H), 1.19 (t, J = 7.0 Hz, 3H), 1.06–1.01 (m, 3H). ES-MS: m/z 629.04 $[M + H]^+$. Elemental analysis calculated: C, 32.63; H, 3.31; N, 4.30; Found: C, 32.55; H, 3.28; N, 4.35.

Data for 2: ^{1}H NMR (500 MHz, d_6-DMSO) δ 9.31 (d, J = 5.1 Hz, 1H), 8.29 (td, J = 7.8, 1.4 Hz, 1H), 7.47 (d, J = 8.0 Hz, 1H), 7.31 (t, J = 4.5 Hz, 1H), 6.86–6.83 (m, 1H), 6.73 (d, J = 7.9 Hz, 1H), 5.99 (d, J = 1.7 Hz, 1H), 5.92 (d, J = 10.5 Hz, 2H), 4.89 (d, J = 20.5 Hz, 1H), 4.19–4.13 (m, 2H), 4.10–4.00 (m, 4H), 3.63 (dd, J = 14.3, 7.2 Hz, 2H), 1.24–1.20 (m, 3H), 1.14 (t, J = 7.0 Hz, 3H). ESI-MS: m/z 643.04 $[M + H]^+$. Elemental analysis calculated: C, 33.72; H, 3.36; N, 4.28; Found: C, 33.65; H, 3.42; N, 4.35.

Data for 3: ^{1}H NMR (500 MHz, d_6-DMSO) δ 9.31 (d, J = 4.5 Hz, 1H), 8.23–8.18 (m, 1H), 7.65 (d, J = 8.0 Hz, 1H), 7.60–7.56 (m, 1H), 6.81–6.79 (m, 2H), 6.67 (dd, J = 7.9, 1.4 Hz, 1H), 5.95–5.94 (m, 2H), 5.14 (d, J = 19.7 Hz, 1H), 4.29 (dt, J = 10.2, 7.0 Hz, 1H), 4.21–4.10 (m, 3H), 3.13 (dt, J = 15.4, 6.6 Hz, 1H), 2.99 (d, J = 3.6 Hz, 3H), 1.26 (t, J = 7.1 Hz, 3H), 1.18 (t, J = 7.0 Hz, 3H). ESI-MS: m/z 657.06 $[M + H]^+$. Elemental analysis calculated: C, 34.40; H, 3.76; N, 4.38; Found: C, 34.45; H, 3.78; N, 4.46.

Data for 4: ^{1}H NMR (500 M Hz, d_6-DMSO) δ 9.30 (d, J = 4.7 Hz, 1H), 8.32–8.22 (td, J = 7.7, 1.6 Hz, 1H), 7.70–7.65 (m, 1H), 7.56 (d, J = 7.9 Hz, 1H), 6.62–6.58 (m, 1H), 6.38 (d, J = 2.5 Hz, 1H), 6.15 (dd, J = 8.6, 2.5 Hz, 1H), 5.03 (d, J = 23.9 Hz, 1H), 4.38–4.22 (m, 2H), 4.18 (m, 1H), 4.11 (m, 1H), 3.98–3.87 (s, 3H), 3.84–3.74 (s, 3H), 1.19 (t, J = 7.0 Hz, 3H), 1.05 (t, J = 7.0 Hz, 3H). ESI + MS: m/z 645.09 $[M + H]^+$. Elemental analysis calculated: C, 33.42; H, 3.73; N, 4.43; Found: C, 33.50; H, 3.75; N, 4.36.

Data for 5: ^{1}H NMR (500 MHz, d_6-DMSO) δ 9.51 (m, 1H), 8.57 (dd, J = 17.3, 5.3 Hz, 1H), 7.84 (d, J = 8.0 Hz, 1H), 7.42 (d, J = 7.9 Hz, 1H), 6.82 (d, J = 9.4 Hz, 1H), 6.79 (d, J = 4.2 Hz, 1H), 6.72 (d, J = 8.3 Hz, 1H), 4.89 (d, J = 20.4 Hz, 1H), 4.55–4.30 (m, 2H), 4.08–4.01 (m, 2H), 3.75 (d, J = 3.6 Hz, 2H), 3.68 (s, 3H), 3.64 (s, 3H), 1.27 (q, J = 6.8 Hz, 3H), 1.02 (t, J = 6.9 Hz, 3H). ESI-MS: m/z 659.07 $[M + H]^+$. Elemental analysis calculated: C, 34.80; H, 3.90; N, 4.35; Found: C, 34.71; H, 3.95; N, 4.32.

Data for 6: ^{1}H NMR (500 MHz, d_6-DMSO) δ 9.40 (dd, J = 40.4, 5.6 Hz, 1H), 8.61 (d, J = 5.6 Hz, 1H), 7.76–7.62 (m, 1H), 6.84 (s, 2H), 6.81 (d, J = 9.4 Hz, 1H), 6.72 (dd, J = 8.0, 1.6 Hz, 1H), 5.15 (d, J = 19.6 Hz, 1H), δ 4.54 (m, 1H), 4.27 (m, 1H), 4.15 (m, 2H), 3.68 (s, 3H), 3.64 (s, 3H), 1.28 (t, J = 7.0 Hz, 3H), 1.02 (t, J = 6.9 Hz, 3H). ESI-MS: m/z 673.12 $[M + H]^+$. Elemental analysis calculated: C, 35.45; H, 4.10; N, 4.28; Found: C, 35.48; H, 4.15; N, 4.23.

4.3.3. X-ray crystallography

The single crystals were mounted on glass fibres, and crystal data were collected on a Agilent SuperNova CCD diffractometer equipped with graphite monochromated Mo Kα radiation (λ = 0.71073 Å) at room temperature. Absorption correction was applied by using the multiscan program SADABS [37]. The structures were solved with direct methods and refined using SHELX-97 programs [38]. The non-hydrogen atoms were located in successive difference Fourier synthesis. The final refinement was performed by full-matrix least-squares methods with anisotropic thermal parameters for non-hydrogen atoms on F^2. The hydrogen atoms were added theoretically and riding on the concerned atoms. The crystallographic data and refinement details of the structures are summarized Table 2.

4.4. Cytotoxicity assay

The cell lines MG-63, SK-OV-3, HepG2 and HL-7702 were obtained from the Shanghai Cell Bank in the Chinese Academy of Sciences. Tumour cell lines were grown in the RPMI-1640 medium supplemented with 10% (v/v) foetal bovine serum, 2 mM glutamine, 100 U/mL penicillin, and 100 U/mL streptomycin at 37 °C, in a highly humidified atmosphere of 95% air/5% CO_2. The cytotoxicity of the title compounds against MG-63, SK-OV-3, HepG2 cell lines was examined by the microculture tetrazolium (MTT) assay [39]. The experiments were carried out using reported procedure [40]. The growth inhibitory rate of treated cells was calculated using the data from three replicate tests as $(OD_{control} - OD_{test})/OD_{control} \times 100\%$. The compounds were incubated with various cell lines for 48 h at five different concentrations of complex dissolved in fresh media; the range of concentrations used is dependent on the complex. The final IC_{50} values were calculated by the Bliss method (n = 5). All tests were independently repeated at least three times.

4.5. Apoptosis assays by flow cytometry assay

The ability of platinum complexes **2**, **5** to induce apoptosis is evaluated in MG-63 cell line using Annexin V conjugated with FITC and propidium iodide (PI) counterstaining by flow cytometry. MG-63 cells of exponential growth were inoculated in 6-well plates and cultured for 12 h before the platinum compounds were added to give the indicated final concentrations. After 48-h incubation, cells were harvested, washed twice in phosphate-buffered saline (PBS), and resuspended in 100 μL binding buffer (including 140 mmol/L NaCl, 2.5 mmol/L $CaCl_2$ and 10 mmol/L Hepes/NaOH, pH 7.4) at a concentration of 1×10^6 cells/mL. Then cells were incubated with 5 μL of Annexin V– FITC (in buffer including 10 mmol/L NaCl, 1% bovine serum albumin, 0.02% NaN_3 and 50 mmol/L Tris, pH 7.4) and 10 μL PI (20 μg/mL) for 15 min at room temperature in the dark. Cells were kept shielded from light before being analyzed by flow cytometry using a Becton–Dickinson FACSCalibur.

4.6. Cell-cycle analysis

MG-63 cell lines were maintained in Dulbecco's modified Eagle's medium with 10% foetal calf serum in 5% CO_2 at 37 °C. Cells were harvested by trypsinization and rinsed with PBS. After centrifugation, the pellet (10^5–10^6 cells) was suspended in 1 mL of PBS and kept on ice for 5 min. The cell suspension was then fixed by the dropwise addition of 9 mL precooled (4 °C) 100% ethanol with violent shaking. Fixed samples were kept at 4 °C until use. For staining, cells were centrifuged, resuspended in PBS, digested with 150 mL of RNase A (250 μg/mL), and treated with 150 mL of propidium iodide (PI) (0.15 mM), then incubated for 30 min at 4 °C. PI-positive cells were counted with a FACScan Fluorescence-activated cell sorter

Table 2
Crystal data and structure refinement details for complexes **1**–**6**.

Formula	$C_{17}H_{21}Cl_2N_2-O_5PPt$	$C_{18}H_{23}Cl_2N_2-O_5PPt$	$C_{19}H_{25}Cl_2N_2-O_5PPt$	$C_{20}H_{31}Cl_2N_2-O_6PPt$	$C_{19}H_{27}Cl_2N_2-O_5PPt$	$C_{20}H_{29}Cl_2N_2-O_5PPt$
fw	630.31	644.34	658.36	692.42	660.39	674.40
T/K	293(2)	293(2)	293(2)	293(2)	293(2)	293(2)
Crystal system	Triclinic	Orthorhombic	Triclinic	Monoclinic	Triclinic	Monoclinic
Space group	*P*-1	*Pbca*	*P*-1	*P*2(1)/*c*	*P*-1	*P*2(1)/*c*
a, Å	9.4727(5)	16.3662(6)	9.0519(4)	11.7240(2)	8.8259(9)	9.0079(2)
b, Å	10.9663(4)	13.8113(6)	11.9167(5)	9.4256(2)	12.0680(12)	11.6889(2)
c, Å	12.1605(5)	19.5612(7)	12.6630(6)	23.4453(4)	12.1806(12)	23.5603(4)
α, °	69.591(4)	90.00	113.756(4)	90.00	96.315(8)	90.00
β, °	68.815(3)	90.00	106.237(4)	93.8117(18)	100.508(8)	97.7882(16)
γ, °	74.327(3)	90.00	99.734(4)	90.00	106.393(9)	90.00
V, Å^3	1088.81(6)	4421.6(3)	1136.99(11)	2585.11(9)	1205.7(2)	2457.82(7)
Z	2	8	2	4	2	4
D_c, g cm^{-3}	1.923	1.936	1.923	1.779	1.819	1.822
μ, mm^{-1}	6.792	6.692	6.509	5.735	6.138	6.021
GOF on F^2	1.000	1.021	1.067	1.094	1.084	1.134
Reflns(collected/unique)	8635/4465	35,945/4511	91,27/4634	20,897/5284	10,060/4914	20,445/5024
R_{int}	0.0333	0.1743	0.0285	0.0313	0.0491	0.0299
R_1[a] ($I > 2\sigma(I)$)	0.0342	0.0616	0.0303	0.0360	0.0381	0.0292
wR_2[b] (all data)	0.0707	0.1919	0.0718	0.1004	0.0861	0.0578

[a] $R_1 = \sum||F_o| - |F_c||/\sum|F_o|$.
[b] $wR_2 = [\sum w(F_o^2 - F_c^2)^2/\sum w(F_o^2)^2]^{1/2}$.

(FACS). The population of cells in each cell-cycle phase was determined using Cell Modi FIT software (Becton Dickinson).

4.7. Agarose gel electrophoresis assay

In plasmid DNA unwinding experiments, all compounds were prepared as 2×10^{-3} M stock solutions of DMSO and diluted to 10 and 100 μM by 1 × TBE buffer. Compounds of various concentrations were mixed with 0.5 μg DNA and made up to a total 25 μL by TBE buffer so that the same experiment can be repeated twice. All samples were incubated at 25 °C in dark for 4 h. Then 12 μL of each sample mixed with 2 μL DNA loading buffer was electrophoresed at 5 V/cm through 0.8% agarose gel immersed in 1 × TBE buffer solution for 60 min. Finally, the gel was stained with EB (1.27 μM) in dark for 30 min, followed by visualized on a BIO-RAD imaging system with a UV–vis transilluminator [41].

4.8. Statistics

The data were processed by the Student's *t*-test with the significance level $P \leq 0.05$ using SPSS 13.0.

Acknowledgements

This work was supported by the National Natural Science Foundation of China (No. 21271051), National Basic Research Program of China (No. 2012CB723501), and Natural Science Foundation of Guangxi Province (Nos. 2010GXNSFF013001, 2012GXNSFDA053005, 2012GXNSFDA385001) as well as "BAGUI Scholar" program of Guangxi of China.

Appendix A. Supplementary data

Supplementary data associated with this article can be found, in the online version, at http://dx.doi.org/10.1016/j.ejmech.2013.01.055.

References

[1] J.J. Wilson, S.J. Lippard, J. Med. Chem. 55 (2012) 5326–5336.
[2] L. Kelland, Nat. Rev. Cancer 7 (2007) 573–594.
[3] P.C. Bruijnincx, P.J. Sadler, Curr. Opin. Chem. Biol. 12 (2008) 197–206.
[4] C.A. Rabik, M.E. Dolan, Cancer Treat. Rev. 33 (2007) 9–23.
[5] M. Frezza, Q.P. Dou, Y. Xiao, H. Samouei, M. Rashidi, F. Samari, B. Hemmateenejad, J. Med. Chem. 54 (2011) 6166–6176.
[6] Z.Q. Xue, M. Lin, J. Zhu, J. Zhang, Y.Z. Li, Z. Guo, Chem. Commun. 46 (2010) 1212–1214.
[7] S.V. Zutphen, J. Reedijk, Coord. Chem. Rev. 249 (2005) 2845–2853.
[8] E. Gabano, M. Ravera, D. Osella, Curr. Med. Chem. 16 (2009) 4544–4580.
[9] F. Kratz, I.A. Muller, C. Ryppa, A. Warnecke, ChemMedChem 3 (2008) 20–53.
[10] Z. Yang, X. Wang, H. Diao, J. Zhang, H. Li, H. Sun, Z. Guo, Chem. Commun. (2007) 3453–3455.
[11] Y.Z. Min, C.Q. Mao, S. Chen, G.L. Ma, J. Wang, Y.Z. Liu, Angew. Chem. Int. Ed. 51 (2012) 6742–6747.
[12] J.R. William, M.P. Kimberly, M.L. Kathryn, W. Lin, J. Am. Chem. Soc. 130 (2008) 11584–11585.
[13] S.D. Brown, P.I. Nativo, J.A. Smith, D. Stirling, P.R. Edwards, B. Venugopal, D.J. Flint, J.A. Plumb, D. Graham, N.J. Wheate, J. Am. Chem. Soc. 132 (2010) 4678–4684.
[14] S. Kaida, H. Cabra, M. Kumagai, A. Kishimura, Y. Terada, M. Sekino, Cancer Res. 70 (2010) 7031–7041.
[15] L.C. Chou, M.T. Tsai, M.H. Hsu, S.H. Wang, T.D. Way, C.H. Huang, H.Y. Lin, K.D. Qian, Y.Z. Dong, K.H. Lee, L.J. Huang, S.C. Kuo, J. Med. Chem. 53 (2010) 8047–8058.
[16] E. Kotsikorou, E. Oldfield, J. Med. Chem. 46 (2003) 2932–2944.
[17] F. Orsini, G. Sello, M. Sisti, Curr. Med. Chem. 17 (2010) 264–289.
[18] S. Piccinonna, N. Margiotta, C. Pacifico, A. Lopalco, N. Denora, S. Fedi, M. Corsinic, G. Natile, Dalton Trans. 41 (2012) 9689–9699.
[19] J. Bird, A.J.M. Williams, S.S. Rahman, R.W. Ward, J. Med. Chem. 37 (1994) 158–169.
[20] E. Naydenova, K. Troev, M.T. Ancheva, G. Hagele, I. Ivanov, A. Kril, Amino Acids 33 (2007) 695–702.
[21] M. Collinsova, J. Jiracek, Curr. Med. Chem. 7 (2000) 629–647.
[22] J.D. Compain, P. Mialane, J. Marrot, F. Cheresse, W. Zhu, E. Oldfield, A. Dolbecq, Chem. Eur. J. 16 (2010) 13741–13748.
[23] I. Kraicheva, A. Bogomilova, I. Tsacheva, G. Momekov, K. Troev, Eur. J. Med. Chem. 44 (2009) 3363–3367.
[24] E. Dabrowska, A. Burzynska, A. Mucha, E.M. Jon, W.S. Dobrowolska, Ł. Berlicki, P. Kafarski, J. Organomet. Chem. 694 (2009) 3806–3813.
[25] I.C. Dormehl, E. Kilian, F.H.A. Schneeweiss, Arzneim. Forsch. 51 (2001) 258–263.
[26] S. Cherenok, A. Vovk, I. Muravyova, A. Shivanyuk, V. Kukhar, J. Lipkowski, V. Kalchenko, Org. Lett. 8 (2006) 549–552.
[27] I.N. Hughes, P.J. O'Brien, D. Herschlag, J. Am. Chem. Soc. 127 (2005) 9314–9315.
[28] Z.-F. Chen, Y.-C. Liu, L.-M. Liu, H.-S. Wang, S.-H. Qin, B.-L. Wang, H.-D. Bian, B. Yang, H.-K. Fun, H.-G. Liu, H. Liang, C. Orvig, Dalton Trans. (2009) 262–272.
[29] J.M. PeÂrez, I.L. Solera, E.I. Montero, M.F. BranÄ, C. Alonso, S.P. Robinson, C.N. Ranninger, J. Med. Chem. 42 (1999) 5482–5486.
[30] S. Hochreuther, R. Puchta, R. Eldik, Inorg. Chem. 50 (2011) 12747–12761.
[31] M. Galanski, S. Slaby, M.A. Jakupec, B.K. Keppler, J. Med. Chem. 46 (2003) 4946–4951.
[32] R. Sasanelli, A. Boccarelli, D. Giordano, M. Laforgia, F. Arnesano, G. Natile, C. Cardellicchio, M.A. Capozzi, M. Coluccia, J. Med. Chem. 50 (2007) 3434–3441.
[33] R.N. Bose, L. Maurmann, R.J. Mishur, L. Yasui, S. Gupta, W.S. Grayburn, H. Hofstetter, T. Salley, Proc. Natl. Acad. Sci. U.S.A. 105 (2008) 18314–18319.

[34] R.S. Dothager, K.S. Putt, B.J. Allen, B.J. Leslie, V. Nesterenko, P.J. Hergenrother, J. Am. Chem. Soc. 127 (2005) 8686–8696.
[35] V. Nesterenko, K.S. Putt, P.J. Hergenrother, J. Am. Chem. Soc. 125 (2003) 14672–14673.
[36] P. Jordana, M.C. Fonseca, Cell. Mol. Life Sci. 57 (2000) 1229–1235.
[37] G.M. Sheldrick, SADABS. Version 2.05, University of Göttingen, Göttingen, Germany, 2002.
[38] G.M. Sheldrick, SHELXS-97, Program for Solution of Crystal Structures, University of Göttingen, Göttingen, Germany, 1997.
[39] M.C. Alley, D.A. Scudiero, A. Monks, M.L. Hursey, M.J. Czerwinski, D.L. Fine, B.J. Abbott, J.G. Mayo, R.H. Shoemaker, M.R. Boyd, Cancer Res. 48 (1988) 589–601.
[40] Z.F. Chen, Y.F. Shi, Y.C. Liu, X. Hong, B. Geng, Y. Peng, H. Liang, Inorg. Chem. 51 (2012) 1998–2009.
[41] M.V. Keck, S.J. Lippard, J. Am. Chem. Soc. 114 (1992) 3386–3390.